ELSEVIER

Biophysical Chemistry 57 (1996) 205–217

Biophysical Chemistry

Molecular dynamics of amphotericin B. II. Dimer in water

Jan Mazerski *, Edward Borowski

Department of Pharmaceutical Technology and Biochemistry, Technical University of Gdańsk, Narutowicza St. 11 / 12, PL80-952 Gdańsk, Poland

Received 21 November 1994; revised 14 February 1995; accepted 27 March 1995

Abstract

Molecular dynamics simulations were performed for a dimer of the antifungal antibiotic, amphotericin B, in water. In the first step of the work three appropriately selected versions of the dimer structure were taken into consideration. In each version antibiotic molecules were placed antiparallel with polar and ionizable groups outside the hydrophobic core formed by polyene chromophores. During short dynamic simulations versions of the dimer structure were compared in respect of the energy of dimerization. The highest energy was observed for the structure in which polyene chromophores superimposed each other as much as possible and this version was subjected to the main simulation. The analysis of 66 snapshot geometries stored during 33 ps dynamic trajectory allowed us to draw three main conclusions: (i) the relative orientation of the amino-sugar moiety and chromophore as well as conformation of the antibiotic macrolide ring were different in both molecules and could exhibit dynamic changes, (ii) the dimer structure exhibited intrinsic asymmetry which could be responsible for characteristic circular dichroism spectra of the aggregated form of the antibiotic, (iii) relatively high stability of the dimer structure resulted not only from hydrophobic interactions between chromophores but also from hydrogen bonds networks that were observed around polar terminals of antibiotic molecules. Implications of these features of the dimer structure for its susceptibility on the ionic state of carboxyl and/or amino groups are also discussed.

Keywords: Molecular dynamics in water; Dimer structure; Antifungal antibiotic; Amphotericin B; Conformational flexibility

1. Introduction

Amphotericin B (AMB), a potent antifungal agent, is a heptaene macrolide produced by *Streptomyces nodosus*. This antibiotic is the main drug used in patients with deep-seated mycotic infections. The increased frequency of organ transplantations and the epidemics of acquired immunodeficiency syndrome (AIDS) are the main reasons for the significant increase of fungal infections observed in the last years. The fungicidal action of AMB is based on its interaction with membrane located ergosterol leading to permeabilizing effects and lethal discharge of ion gradients.

The AMB molecule has a large lactone ring, one side of which is a non-polar conjugate heptaene, while the other side is polar, owing to the presence of hydroxyl groups (Fig. 1). An amino-sugar mycosamine is attached to the macrolide ring by a glycoside bond. Thus, the molecule is amphiphilic. It is also amphoteric, due to the presence of a carboxyl and an amino group, both of which are charged at

* Corresponding author.

SSDI 0301-4622(95)00062-3

physiological pH. These molecular characteristics provoke AMB to form aggregates in aqueous media and decrease its solubility. The poor water solubility of this antibiotic is one of the important factors limiting its application in the therapy of systemic fungal infections [1]. However, the main disadvantage of AMB is its high animal toxicity.

Recent studies show that toxic effects of AMB depend on its aggregation state in vitro [2–4] as well as in vivo [3,5,6]. The examination of this phenomenon might be of importance for the design of a modified antibiotic with decreased toxicity.

In aqueous media optical absorption as well as circular dichroism (CD) spectra of AMB are concentration-dependent [7]. At very low concentration in water ($c < 10^{-7}$ M) the spectrum indicates the existence of the antibiotic in monomeric form. As the concentration increases, spectra manifest changes typical for aggregates formation and above $c = 10^{-4}$ M the monomeric form is spectroscopically undetectable. The changes in the CD spectrum as a function of concentration are consistent with the formation of small oligomers, most probably dimers [8–11]. In contrast, differential ultrafiltration [10] and light scattering experiments [12] indicate that large species of molecular weight up to 10^6 dalton exist at AMB concentration above 10^{-5} M in aqueous media. The comparison of the results obtained by circular dichroism and light scattering techniques in hydroalcoholic media suggest [12] that the formation of large, insoluble aggregates detected by the light scattering is not reflected in the spectroscopic properties.

On the basis of experiments concerning influence of the ionic state of the AMB molecule on the aggregation behaviour we have proposed a multi-step model of polyene antibiotic self-association [11]. In this model we take into consideration the fact that polyene antibiotic solutions in aqueous media contain many different species with a molecular weight in the range of one thousand (monomer) to a few million (colloid type micelles). Molecules of AMB in the monomeric state are amphiphilic and in aqueous medium have a strong tendency to reduce the surface of apolar parts exposed to water. The straight way to this reduction is interaction with other monomeric molecules. Thus, dimerization of monomers to more hydrophilic dimers should be a first step in aggregation. Formed dimers may subsequently interact to continue diminishing of hydrophobicity by formation of hydrophilic, colloid-type micelles. The first step (dimerization) is responsible for spectroscopic changes, the next ones (micellization) are not reflected in spectroscopic properties of the solution. It may suggest that the micelle structure is chaotically organized and the environment of the chromophores is not changed during this process. We experimentally showed that net charge of the AMB molecule has a strong influence on the structure of the dimer as well as on dimer and micelles formation constants [11].

There is no experimental evidence of the structure of the dimers or other aggregates. A few hypotheses concerning three-dimensional arrangement of the antibiotic molecules forming an aggregate have been proposed [8,13,14]. All of them were based on the analysis or modelling of the spectroscopic properties (UV and/or CD spectra) of the aggregates.

Ernst and co-workers obtained the best reproducibility of UV spectrum for dimers in which chromophores (double bonds) were located antiparallel in the distance of 0.6 nm [8]. For sufficient reproduc-

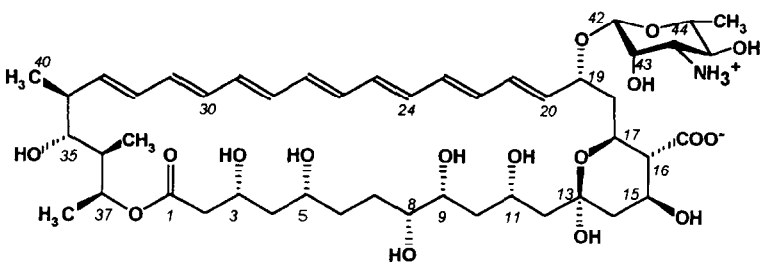

Fig. 1. Structure of amphotericin B (AMB).

tion of the CD spectrum a distance between helix forming dimers should be equal to 1.1 nm and two neighbouring dimers should be twisted 170°.

In the model of Hemenger et al. [13] the chromophores were located antiparallel at 0.49 nm. The distance between chromophores along an axis of the helix was determined on 0.29 nm. Neighbouring dimers should be twisted 46°.

Barwicz et al. have proposed a totally different arrangement of the AMB molecules in the aggregates [14]. This model was based only on the analysis of absorption spectra of the monomer and aggregate solutions. According to this model a few antibiotic molecules were organized in a form of tube-like hydrophilic species. Chromophores were stacked parallelly inside the aggregate and surrounded by hydrophilic parts of AMB molecules. Geometrical parameters of the model depend on a number of molecules forming the cylindrical micelles. Authors revealed that spectra can be adequately reproduced for aggregates containing 4 to 8 AMB molecules. The distance between neighbouring chromophores only slightly depends on the number of molecules and varies from 1.33 to 1.4 nm. A radius of chromophore tube was more dependent on the number of molecules. It varies from 0.94 nm in the tetramer to 1.83 nm in the octamer. Tube-like micelles could also associate in the 'head-to-tail' pattern. A distance between centers of the micelles was evaluated at 2.7 nm. However, this interesting model is in contradiction with experimental results mentioned above [8–11] concerning formation of the dimers.

Such important discrepancies between molecular organization of the aggregates proposed on the basis of spectroscopical properties indicate that a new approach to this problem is necessary. The mechanism of aggregation of amphiphilic molecules in an aqueous medium is a very complicated one in which hydrophobic and polar substituents play their parts with a delicate balance between the attractive and the repulsive forces. In our opinion molecular dynamics simulation could be one of the approaches which may solve this problem. In addition, results of molecular dynamics simulations of the AMB single molecule [15] strongly suggest that the dynamic behaviour of the molecule could be an important factor determining the structure of the aggregate. The results of molecular dynamics simulation of AMB dimer obtained in presence of water molecules are a subject of this paper.

2. Procedures

For the energy minimizations and molecular dynamics simulations the GROMOS software package was used (W.F. van Gunsteren and H.J.C. Berendsen, BIOMOS B.V., Laboratory for Physical Chemistry, University of Groningen, The Netherlands). The integration of the classical equations of motion was done with a time step of 2 fs with bond lengths constrained with 10^{-3} relative to their standard values by using the SHAKE algorithm [16]. The energy function was composed of bonding terms represent-

Table 1
Averaged energies, in kJ/mol, of intermolecular interactions during the last 0.5 ps period of dynamic relaxation of different versions of dimer geometry. Energies of interactions between single AMB molecule and water are also presented for comparison

Interaction type	Dimer version			Single AMB molecule [15]
	A	B	C	
AMB-AMB				
Lennard-Jones	−157 ± 4	−157 ± 9	−59 ± 9	
Electrostatic	−8 ± 4	−31 ± 5	1 ± 1	
Association energy	165 ± 4	188 ± 8	58 ± 8	
AMB-water				
Lennard-Jones	−600 ± 25	−580 ± 25	−730 ± 20	−320 [a] ± 30
Electrostatic	−2420 ± 55	−2620 ± 65	−2510 ± 50	−2770 [a] ± 150
Hydration energy	3020 ± 50	3200 ± 60	3240 ± 45	3100 [a] ± 140
Dimerization energy	3185 ± 50	3390 ± 60	3300 ± 50	

[a] Calculated for two single molecules.

ing internal topology as bond lengths, bond angles, torsion angles, improper dihedrals, as well as non-bonded terms consisting of van der Waals interactions and electrostatic contributions. For all calculations, the standard GROMOS force field was used. No explicit hydrogen bond function was employed in this force field.

The initial coordinates for the antibiotic molecule were obtained from atomic X-ray coordinates for heavy atoms [17]. AMB molecules were in a form of zwitter-ion with dissociated carboxyl and protonated amino groups. Hydrogen atoms bound to the carbon atoms were considered as 'united atom' representations. Hydrogens bound to oxygen and nitrogen atoms were placed following the standard geometry of hydroxyl group and ammonium cation, respectively.

The initial coordinates for different geometries of the dimer were prepared by superimposing coordinates for AMB molecules arranged according to the version upon the coordinates of a well-'aged' rectangular box of water molecules equilibrated in a previous simulation of pure SPC water. Those water molecules with oxygen atoms whose Van der Waals radii overlapped any of the atoms in the AMB

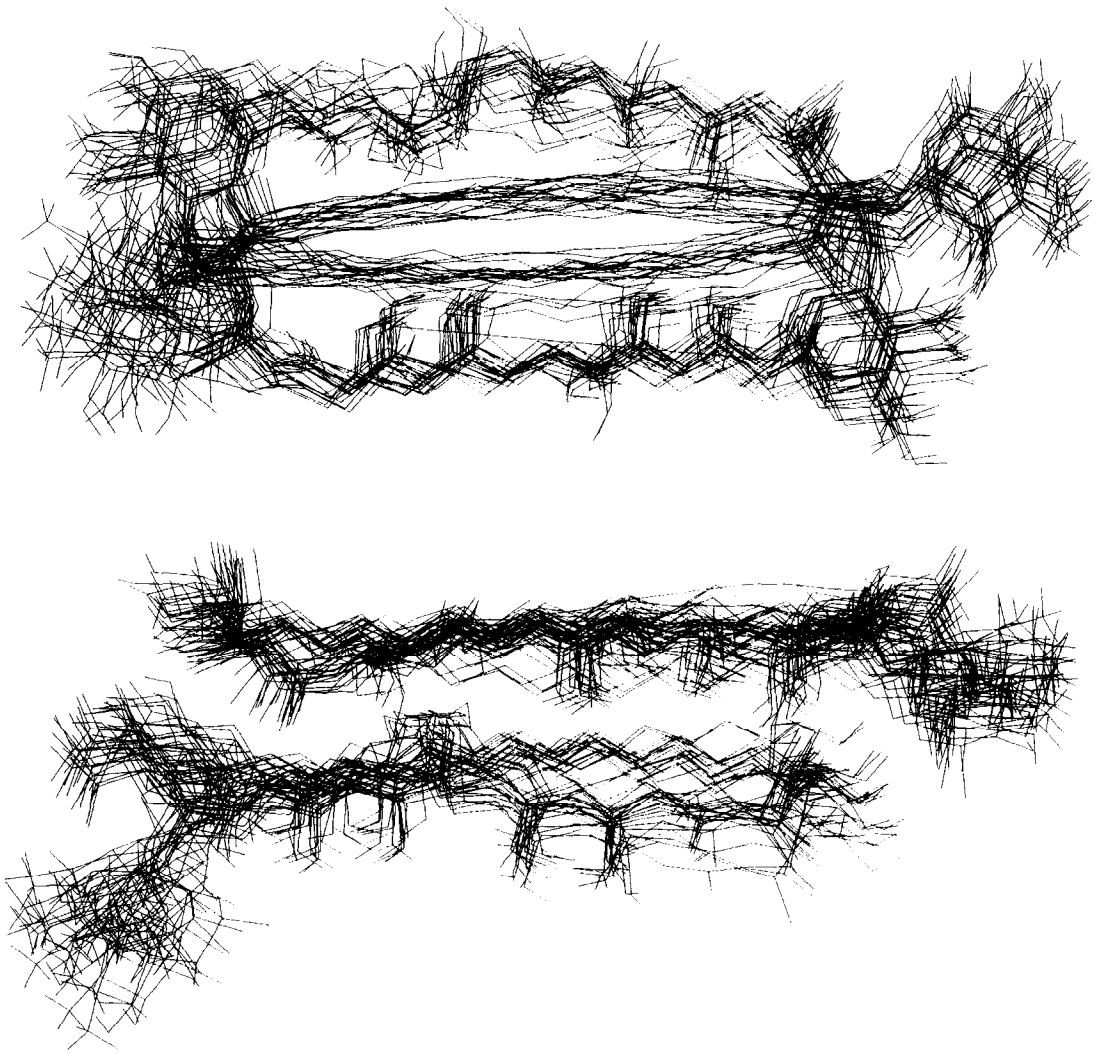

Fig. 2. Orthogonal views of 21 snapshots taken from the dynamic run every 1.5 ps.

molecule were then discarded from the system. The box edges were watched in such manner that minimum distance between each of the dimer atoms and walls of the box was higher than 0.5 nm. Minimum image periodic boundary conditions were employed, and interactions between charge groups greater than 0.8 nm apart were truncated. The list of non-bonded interactions was updated every 10 steps of calculation.

After 100 steps of energy minimization each version of the dimer geometry was equilibrated for 10 ps to relax any artificial starting conditions produced by the initialization procedure, with periodic scaling of the atomic velocities after each 0.5 ps period if the temperature deviated from the desired value of 300 K by more than 10°. During the final 0.5 ps period of equilibration different interaction energies were averaged and stored for analysis. Such protocol has been used by other authors for shortening the equilibration period [18,19].

Following the equilibration period, the simulation for the energetically favoured version of the dimer structure was continued for an additional 33 ps. The temperature was kept at 300 K by coupling the kinetic energy of the system to a heat bath with a relaxation time of 100 fs [20]. Snapshot geometries and energies were stored after each 0.5 ps interval of the simulation.

3. Results

3.1. Selection of the dimer structure

The main problem in molecular mechanics as well as molecular dynamics calculations of multimolecular systems is how to choose the starting arrangement of the system. The typical solution of this problem is to use geometry from crystallographic data. Unfortunately, there are no such data for the dimer of AMB. In this situation we decided to use three different starting geometries. In all geometries AMB molecules were oriented antiparallel and in such manner that polar parts of molecules were outside of dimer. The first geometry (version A) was based on crystallographic data of the N-iodoacetyl derivative [17]: the arrangement of both AMB molecules was the same as the two neighbouring

Table 2
Dynamically averaged dihedral angles of AMB molecules forming the dimer. Dihedral angles which mean values were significantly different in both molecules are presented only

Dihedral angle	AMB′		AMB″		Difference
	Value	RMSF	Value	RMSF	
Macrolide ring					
O37–C1–C2–C3	284.8	17.1	164.7	27.6	120.1
C1–C2–C3–C4	192.3	12.8	174.4	12.5	17.9
C3–C4–C5–C6	185.9	16.1	170.2	13.5	15.7
C5–C6–C7–C8	181.9	11.7	104.4	55.1	
			67.9	10.7	
			182.5	11.7	
C7–C8–C9–C10	173.3	9.2	298.7	10.5	−125.4
C9–C10–C11–C12	172.2	8.3	137.5	46.4	
			169.5	9.8	
			74.9	17.8	
C10–C11–C12–C13	164.3	11.9	184.5	12.5	−20.2
C16–C17–C18–C19	147.5	8.4	168.8	9.2	−21.3
C32–C33–C34–C35	145.3	17.7	114.6	17.0	30.7
C36–C37–O37–C1	−123.2	14.0	−98.1	15.9	−25.1
Relative orientation of mycosamine					
C19–O19–C42–O42	235.2	11.7	267.7	17.6	−32.5
C20–C19–O19–C42	124.2	8.9	107.8	19.4	16.4

molecules in the crystal. Version B was obtained by molecular modelling of the dimer with the requirement that chromophores were superimposed as much as possible. In this geometry the Van der Waals forces should be maximal and the hydrophobic forces minimal. Version C was obtained from geometry B by translation of one of the molecules along the chromophore axis. In this version one end of each chromophore may be in contact with water molecules. This version was used as control. We expected that increase of the surface of apolar parts in contact with water should result in decrease of dimerization energy.

Each of the versions of the dimer geometry were placed in the center of rectangular box filled with SCP water molecules. The number of water molecules depended on the dimensions of box and was equal to 703, 461, and 610, for the respective version orders. During energy optimizations and dynamics simulations the periodic boundary conditions were used. After energy minimization each version of the dimer geometry was equilibrated for 10 ps with periodic scaling of the atomic velocities during this period. During the final 0.5 ps period of equilibration different interaction energies were calculated and averaged.

Two kinds of interaction energies were derived from the data: association energy defined as the interaction between antibiotic molecules which formed the dimer and hydration energy defined as

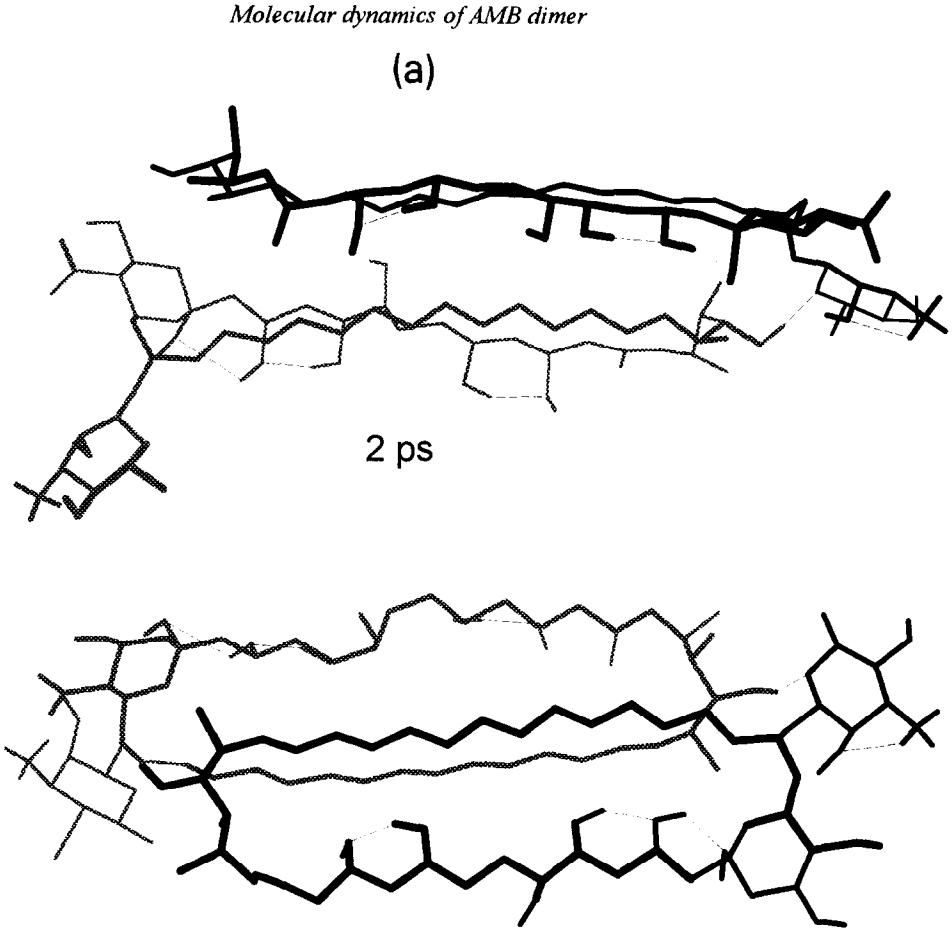

Fig. 3. Orthogonal views of two snapshots representative for conformers of AMB molecules forming the dimer: AMB′ in black, AMB″ in gray. Dashed lines display hydrogen bonds.

the interaction between water and antibiotic molecules. Dimerization energy was defined as the sum of these energies. Averaged values of association, hydration, and dimerization energy for all three versions of the dimer geometry are shown in Table 1. The hydration energy of single AMB molecule [15] is also presented in this Table for comparison. To the next step of the calculation version B which was characterized by the highest dimerization energy was chosen.

3.2. Dynamic behavior of the dimer structure

Initial calculations which have been described in Section 3.1. indicate that version B of starting dimer geometry results in the most energetically favoured structure of the dimer (Table 1). The main dynamics simulation (33 ps) concerned this geometry. The last geometry of the version B trajectory was used as starting geometry for the main simulation with atom velocities taken from Boltzmann's distribution at 300 K. During this simulation the system was weakly coupled to a 300 K thermal bath with time constant of 0.1 ps. Snapshot geometries and energies were stored after each 0.5 ps interval of the simulation. No systematic drift nor jumps of total, kinetic and potential energies were observed during main simulation. Thus, conformers observed during the simulation could be interpreted as species that coexist in equilibrium.

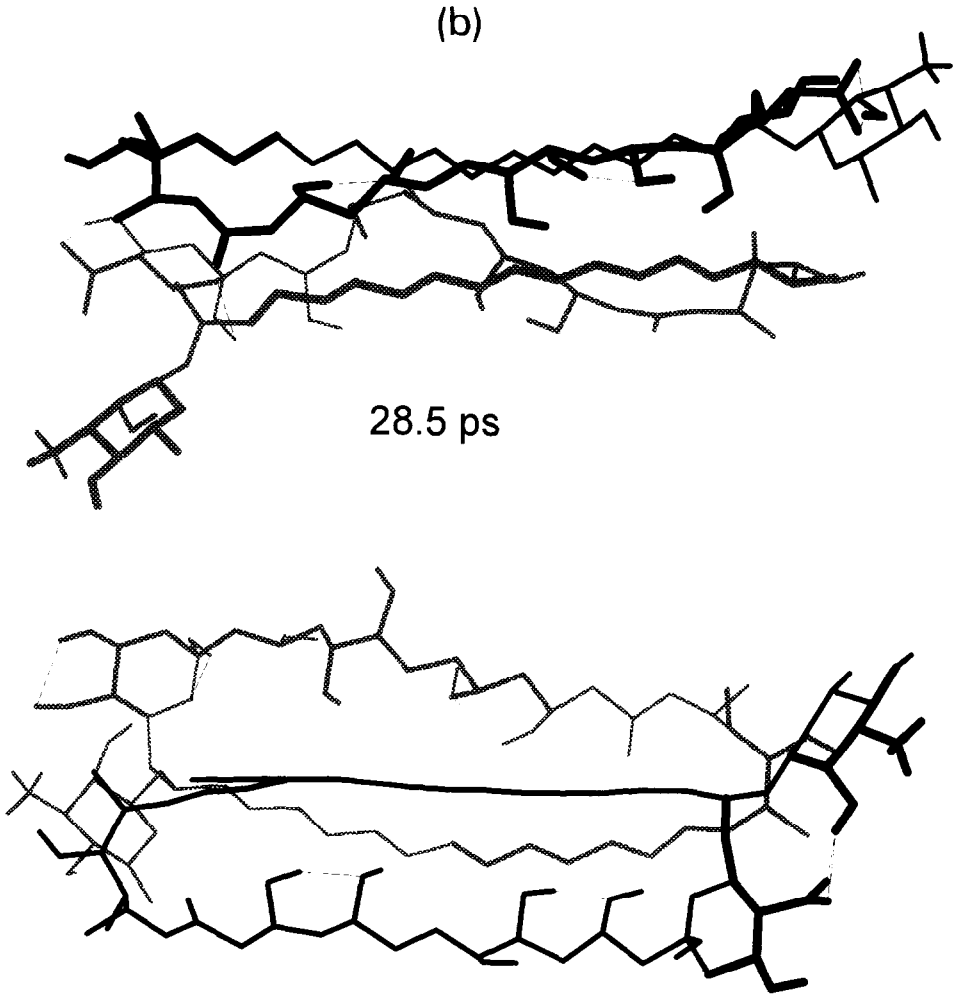

Fig. 3 (continued).

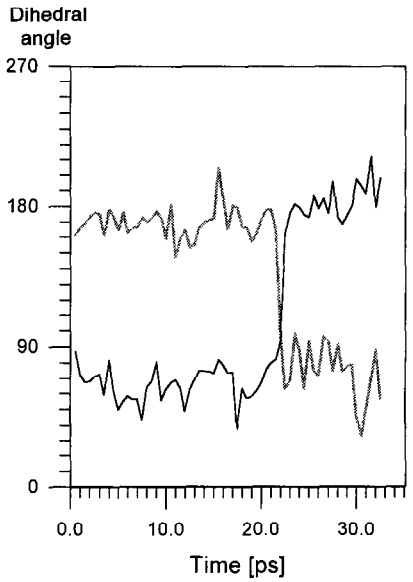

Fig. 4. Histories of AMB″ dihedral angles C5–C6–C7–C8 (black) and C9–C10–C11–C12 (gray) during dynamic simulation.

Architecture of the dimer

Mean planes of the macrolide ring of both AMB molecules forming the dimer are near parallel. The mean value of the angle between that planes during the main simulation was equal to 9.9° ± 5.0° (Fig. 2). Chromophores of both AMB molecules were not exactly antiparallel: the mean value of an angle between long axis of chromophores was equal to 171.0° ± 2.2° and differs significantly from 180°. Relative orientation of chromophore mean planes varied during the simulation from 0° to 90°. The dynamically averaged angle between mean planes of the chromophores was equal to 37.8° ± 21.4°. The distance between centers of chromophores was near constant and its mean value was equal to 0.494 ± 0.029 nm.

Structure of the dimer components

The mean structures of both AMB molecules forming the dimer, as measured by their dynamically averaged dihedral angles, are compared in Table 2. The structure of the mycosamine ring is stable during the simulation time and the same in both molecules. On the contrary, the orientation of the mycosamine moiety in relation to the macrolide ring, as measured by torsion angles C19–O19–C42–O42 and C20–C19–O19–C42, was different in both molecules of AMB. Cumulative effect of these dif-

Table 3
Comparison of intramolecular hydrogen bonds observed in AMB molecules forming the dimer. Hydrogen bonds which cumulative time of existence is longer than 10% of the simulation period are presented only

Hydrogen bond	Cumulative existence time (%)		
	AMB′	AMB″	Between
O3–H3 → O5	83	22	
O5–H5 → O3	14	34	
O9–H9 → O11	94	45	
O11–H11 → O13	82	19	
O13–H13 → O11		33	
O15–H15 → O412		39	
O43–H43 → O411	83		
O35″–H35″ → O42′			17

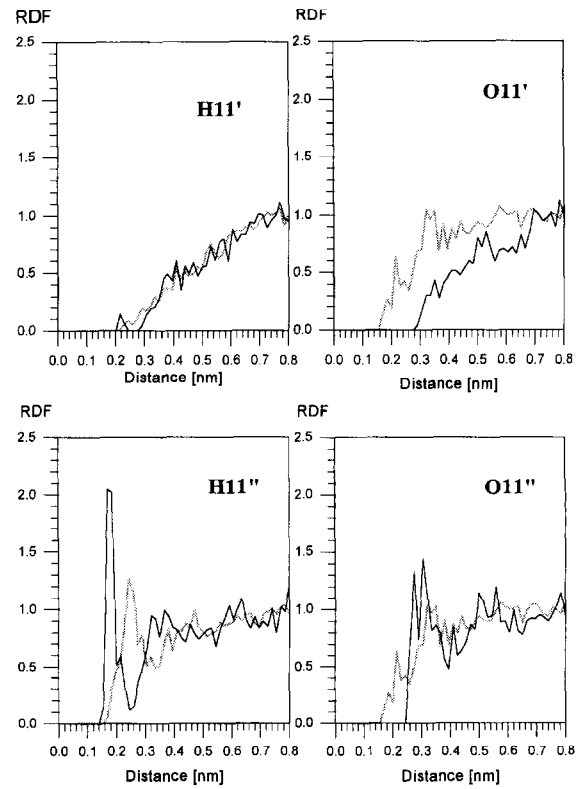

Fig. 5. Radial distribution functions (RDFs) of water oxygen (black lines) and hydrogen (gray lines) atoms around 11-OH groups in both AMB molecules forming the dimer.

ferences results in totally different relative orientation of the amino-sugar moiety in each of the AMB molecules (Figs. 2 and 3): in AMB′ the mycosamine moiety lays practically in the mean plane of the macrolide ring while in AMB″ the amino-sugar ring is almost perpendicular to the plane.

Conformations of the macrolide ring in both AMB molecules forming the dimer also differ significantly (Table 2). The largest differences, about 120°, are observed for torsion angles O37–C1–C2–C3 and C7–C8–C9–C10. Also some other torsion angles in the polyol fragment of the antibiotic molecules differ significantly in both molecules. Moreover, for dihedrals C5–C6–C7–C8 and C9–C10–C11–C12 in AMB″ two distinct conformational states could be observed. Fig. 4. presents histories of these dihedrals. It is noteworthy that transition between two states occurred cooperatively for both torsion angles. It means that the fragment from C7 to C10 with hydroxyl groups at C8 and C9 changes its orientation in relation to the rest of the macrolide ring (Figs. 3a and 3b, respectively). Similar cooperative reorienta-

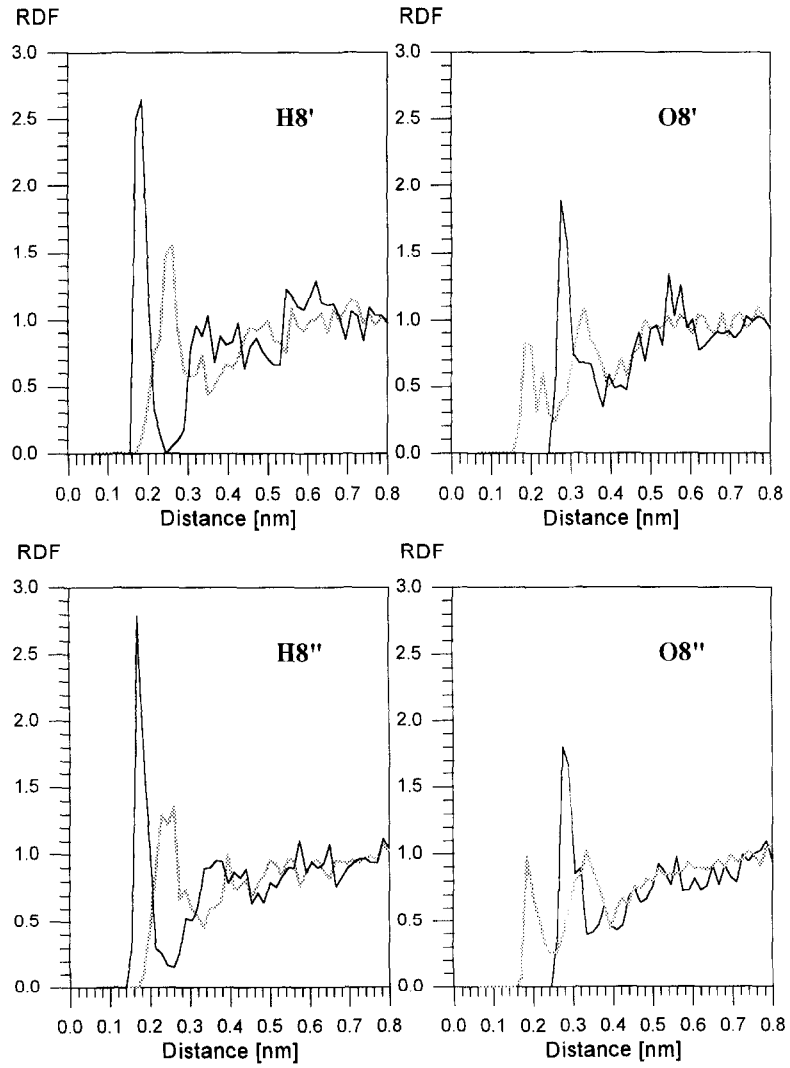

Fig. 6. RDFs of water oxygen (black lines) and hydrogen (gray lines) atoms around 'equatorial' 8-OH groups in both AMB molecules forming the dimer.

tion could be observed in the case of chromophores in both molecules. However, changes of the orientation of the mean plane of chromophore in relation to the mean plane of the remaining part of the macrolide ring were quick and their characteristic suggests rather free rotation then transition between distinct states. The dynamically averaged values of angles between the mean plane of the chromophore and mean plane of the macrolide ring were the same for both molecules and equal to 65.0 ± 17.4° and 56.8° ± 17.6°, respectively.

3.3. Hydrogen bond network

Immutability of AMB molecules' orientation in contrary to local flexibility of their parts suggests existence of some forces responsible for stability of the dimer architecture. One of factors which may play an important role in the stabilization of the dimer general structure may be formation of hydrogen bonds networks. Also asymmetry observed in the conformations of both AMB molecules may be a result of intra- and intermolecular hydrogen bonds networks.

Intramolecular hydrogen bonds detected during simulation are shown in Table 3. Only one hydrogen bond between AMB molecules was detected and it is also shown in this Table. Results presented in Table 3 confirm the existence of the asymmetry between constituents of the dimer. Stable (more than 80% of the simulation time) hydrogen bonds between three pairs of macrolide ring hydroxy groups predominates in one of them (AMB′). In this molecule stable hydrogen bonds between mycosamine 43-OH and carboxyl group is also observed. In contrast, in the second molecule (AMB″) more, but not so stable hydrogen bonds are observed. Surprisingly, in this molecule there was no hydrogen bond detected between mycosamine and the carboxyl group.

The asymmetry between both AMB molecules can also be found on the basis of hydrogen bonds between AMB and water molecules. For example, the 11-OH′ group does not form hydrogen bonds with water molecules. In contrast, 11-OH″ forms such bonds with 5 water molecules. Similar, however, not so strong asymmetry could be observed for 9- and 13-OH groups in both molecules. Radial distribution functions [21] (RDFs) for the 11-OH′ group indicate that water molecules have difficulty in access to this group (Fig. 5). It is noteworthy that the hydrogen atom of this group is practically hidden from interaction with water molecules while the oxygen atom was slightly more accessible. In contrary, hydrogen atoms of 11-OH″ group exhibits RDFs typical for easy accessible, hydrogen bond forming atoms. The oxygen atom of this group is significantly less accessible.

'Equatorial' 8-OH groups of both AMB molecules do not participate in intramolecular hydrogen bonds. These groups took part in the formation of hydrogen bonds with water molecules (Fig. 6). A characteristic feature of RDFs for oxygen atoms of these groups is the low intensity of the first and second maxima of water hydrogen distributions. The first maxima at 0.2 nm are sharp but of low intensity (RDF < 1). Their position corresponds to the typical length of hydrogen bonds in which water molecules are bond donors. The second maxima could be found at 0.31 nm but their intensities are also low. First, maxima of water oxygen distribution could be observed at 0.27 nm. They are sharp and relatively high (RDF ≈ 2.0). Hydrogen atoms of these groups are easy accessible, particularly for water oxygens. Such patterns of radial distribution functions are typical for hydroxyl groups attached to carbon atoms of second or third order.

The existence of intermolecular hydrogen bonds between the mycosamine ring oxygen atoms O42′ and the 35-OH groups of AMB″ (Table 3, Fig. 3a) stabilizes the dimer structure. It is possible only due to the particular orientation of the mycosamine moiety in AMB′. This orientation differs from the crystal one [17] and in our opinion results from the presence of a stable hydrogen bond between 43-OH and the carboxyl group of AMB′ (Table 3, Fig. 3b). In the AMB″ molecule, in which no hydrogen bonds between amino-sugar moiety and the carboxyl group is detected, the orientation of amino-sugar is similar to that found in the crystal and during dynamics simulations of the single molecule [15].

Detailed analysis of the hydrogen bonds between AMB molecules forming the dimer and molecules of water reveals existence of water molecules which interact with two or more different polar atoms or groups of the antibiotic. Such interactions observed for more than 10% of the simulation run are listed in

Table 4
Water mediated interactions between polar atoms of AMB molecules forming the dimer

AMB′	AMB″	Between
O5 ⇔ H5	H3 ⇔ H5	O35′ ⇔ O411″ [a]
O15 ⇔ O412 [a]	H11 ⇔ H13 [a]	O35′ ⇔ O412″ [a]
O35 ⇔ H35	O13 ⇔ O411	H35′ ⇔ O412″
O411 ⇔ O412	O411 ⇔ O412	
	H441 ⇔ H442	

Only interactions in which mediated water molecules form hydrogen bonds by more than 10% of the simulation time are presented. Interactions marked by an asterisk were formed by different water molecules.

Table 4. Except typical situations in which water molecules mediate in interactions between two neighbouring groups one can also find water-mediated interactions between distant groups, for example 13-OH and carboxyl groups in AMB″. Moreover, some water molecules mediate in interactions between AMB molecules. Such interactions are observed between 35-OH of AMB′ and the carboxyl group of AMB″.

4. Discussion

Results presented in Table 1 indicate that dimerization driving-forces originate from hydrophobic interactions as well as from attractive interactions between AMB molecules forming the dimer. The optimal dimer geometry is characterized by significant participation of electrostatic forces in association energy. Detailed analysis of intermolecular interactions presented in Section 3.3 supports this observation: electrostatic interactions between AMB molecules, direct or mediated by water molecules, stabilize the dimer and are responsible for its specific architecture. Near antiparallel arrangement of AMB molecules arises not only from interactions between rigid chromophores but also from stabilizing effects of hydrogen bonds networks which exist between polar terminals of the antibiotic molecules. The key fragment of one such network is formed by the terminal 35-OH″ group and amino-sugar oxygen O42′ (Table 3, Fig. 3a). Intramolecular hydrogen bonds between 43-OH′ and the carboxyl group of the AMB′ as well as between carboxyl group and 15-OH′ supported by hydrogen bonds with water molecules complete this network. On the opposite side of the dimer, water-mediated interactions between 35-OH′ and the carboxyl group of the AMB″ form the second network (Table 4). Geometries of these networks determine, in our opinion, the stability and the architecture of the dimer. Derivatization of amino and/or carboxyl groups as well as changes in their ionic state might result in totally different geometry of above mentioned networks and, as a result, in different architecture of the dimer. Our earlier observation that formation of the dimer as well as of higher associates strongly depends on the net charge of the AMB molecule [11] can now be explained easily. Also other our observation that short-wavelength part of the absorption spectrum of the aggregated form of AMB is affected by the ionic state of the amino and carboxyl groups [11] could be understood in the light of above discussion.

The key spectroscopic feature of the aggregated form of AMB is its very strong excitonic doublet in the circular dichroism spectrum [7]. It is postulated that this doublet is a result of highly asymmetric (helical) arrangement of non-asymmetric dimers [8,13]. However, there are some evidences that the asymmetry is originated on the level of dimer or on other small aggregate [9–11]. The architecture of the dimer obtained as a result of our molecular dynamics simulation differs from previous molecular models of the dimer which were proposed on the basis of circular dichroism and absorption spectra in one point: the long axis of chromophores are neither parallel [14] nor antiparallel [8,13] but form an angle of about 170°. It is interesting that the same value was proposed by Ernst and co-workers [8] as the angle between two neighbouring dimers. The dynamically averaged distance between centers of chromophores is equal to 0.49 nm and is in good agreement with the value proposed by Hemenger and co-workers [13]. Thus, we suggest that the strong excitonic doublet in circular dichroism spectrum does not result from asymmetric arrangement of dimer but from intrinsic asymmetry of the dimer architecture. It is interesting to note that structure of AMB dimer in DMSO proposed by Balakrishnan and Easwaran on the base of 2D NMR [22] is in part similar to this

obtained by us from dynamic simulation. The main difference is that the dimer in DMSO seems to be intrinsically symmetric. Also the CD spectrum of the dimer in DMSO does not exhibit a typical excitonic doublet. In the structure proposed for this dimer two symmetric intermolecular hydrogen bonds between the 35-OH group of one molecule and O42 group of second molecule are crucial for molecular arrangement of the dimer. In contrary to water, the DMSO molecule cannot mediate in the interactions. Moreover, in DMSO the hydrophobic driving-force is not so strong as in water. Both these facts may explain differences in the geometry of dimers in these two solvents.

Since the work of Rinnert and Maigret [23] the macrolide ring of the AMB has been considered as a relatively rigid part of the molecule with only one low-energy and environment independent conformation. In our previous paper [15] we first suggested that the macrolide ring could exist in different conformational states depending on intra- and intermolecular interactions existing in the system. Present work corroborate this suggestion: both molecules forming the dimer have different conformations of the macrolide ring. Moreover, in one of them, AMB″, the ring exists in two different conformations. Both conformers of AMB″ are in equilibrium at 300 K and can mutually transform. However, it should be emphasized that conformational changes of the macrolide ring do not affect the overall rectangular shape of the ring determined by the geometry of the system of seven conjugated double bonds in all-*trans* conformation. Nevertheless conformational changes of the macrolide ring determine the ability of particular polar groups (carbonyl, hydroxyl) to interaction with other groups or molecules. This susceptibility of AMB to form species with the same shape but different local and/or global affinity could explain its tendency to self-association as well as to interactions with molecules of different shape and characteristics: proteins, phospholipids, sterols, and polar organic solvents. During modelling of such complexes not only different conformational states of the antibiotic molecule but also their dynamic transitions should be taken into consideration.

The results presented in this paper as well as in the work of Balakrishnan and Easwaran [22] suggest that the terminal hydroxyl group (35-OH) plays an important role in the formation of AMB dimers. It seems that chemical modifications which diminish or destroy its ability to hydrogen bond formation may result in increasing the solubility of the antibiotic and decreasing its toxicity.

Acknowledgements

This study was supported by the State Committee for Scientific Research, Warsaw, Poland, grant No. 2 P 303 060 06.

References

[1] H.A. Gallis, R.H. Drew and W.W. Pickard, Rev. Infect. Dis., 12 (1990) 308.
[2] I. Gruda, E. Gauthier, S. Elberg, J. Brajtburg and G. Medoff, Biochem. Biophys. Res. Comm., 154 (1988) 954.
[3] I. Gruda, E. Milette, M. Brother, G.S. Kobayashi, G. Medoff and J. Brajtburg, Antimicrob. Agents Chemother., 35 (1991) 24.
[4] J. Bolard, P. Legrand, F. Heitz and B. Cybulska, Biochemistry, 30 (1991) 5707.
[5] J. Barwicz, R. Gareau, A. Audet, A. Morisset, J. Villiard and I. Gruda, Biochem. Biophys. Res. Commun., 181 (1991) 722.
[6] J. Barwicz, S. Christian and I. Gruda, Antimicrob. Agents Chemother., 36 (1992) 2310.
[7] J. Bolard, M. Seigneurt and G. Boudet, Biochim. Biophys. Acta, 599 (1980) 280.
[8] C. Ernst, J. Grange, H. Rinnert, G. Dupont and J. Lematre, Biopolymers, 20 (1981) 1575.
[9] J. Mazerski, J. Bolard and E. Borowski, Biochim. Biophys. Acta, 719 (1982) 11.
[10] G. Strauss and F. Kral, Biopolymers, 21 (1982) 459.
[11] J. Mazerski, J. Grzybowska and E. Borowski, Eur. Biophys. J., 18 (1990) 159.
[12] H. Rinnert, C. Thirion, G. Dupont and J. Lematre, Biopolymers, 16 (1977) 2419.
[13] R.P. Hemenger, T. Kaplan and L.J. Gray, Biopolymers, 22 (1983) 911.
[14] J. Barwicz, W.I. Gruszecki and I. Gruda, J. Colloid Interface Sci., 158 (1993) 71.
[15] J. Mazerski and E. Borowski, Biophys. Chem., 54 (1995) 49.
[16] J.P. Ryckaert, G. Cicotti and H.J.C. Berendsen, J. Comput. Phys., 23 (1977) 327.
[17] P. Ganis, G. Avitabile, W. Mechliński and C.P. Schaffner, J. Am. Chem. Soc., 93 (1971) 4560–4564.

[18] P.H. Axelsen, C. Haydock and F.G. Prendegrast, Biophys. J., 54 (1988) 249.
[19] R.M. Venable, B.R. Brooks and F.W. Carson, Proteins, 15 (1993) 374.
[20] H.J.C. Berendsen, J.P.M. Postma, W.F. van Gunsteren, A.D. Nola and J.R. Haak, J. Chem. Phys., 81 (1984) 3684–3690.
[21] P.J. Rossky and M.J. Karplus, J. Am. Chem. Soc., 101 (1979) 1913.
[22] R.A. Balakrishnan and K.R.K. Easwaran, Biochim. Biophys. Acta, 1148 (1993) 269.
[23] H. Rinnert and B. Maigret, Biophys. Biochem. Res. Commun., 101 (1981) 853.